Calibration of the SHMS Cherenkovs (HGC & NGC)

Ryan Ambrose, Garth Huber
University of Regina

Friday 25 August, 2017

Abstract

The calibration and efficiency of the SHMS Heavy Gas and Noble Gas Cherenkovs (HGC/NGC) are described for run 488. The calibration is determined using two strategies: quadrant and tracksfired. Quadrant uses post-replay processing to divide the Cherenkov signals into separate regions to isolate the single photoelectron peak (SPE). This peak is then used to give the calibration, with a second estimate based off the resultant spacing. Tracksfired uses inherent cuts in hcana to isolate the SPE, then follows the same procedure. The efficiencies of the Cherenkovs are determined by taking the ratio of calibrated data with and without a NPE cut.

1 Introduction

This document details the methodology and resulting calibration of the SHMS Cherenkovs for data collected in the Spring run of 2017. The specific run analyzed is run 488, corresponding to log entries 3467029[1] & 3467038[2]. The running conditions were a central SHMS momentum of 3 GeV/c, carbon 0.5% target white spectrum, with HGC and NGC filled with CO_2 at 1 atm. Of interest at present are scripts that process a replayed run using hcana. It is important to realize this introduces inherent cuts/selection rules to all subsequent analysis. The details of these cuts can be examined in the hcana/src directory, for example the cuts used with the HGC can be found in the CoarseProcess and FineProcess methods in the file THcCherenkov.cxx with the specific parameters in hallc_replay/PARAM/SHMS/HGCER/CUTS/phgcer_cuts.param.

As a brief summary, CoarseProcess uses only Cherenkov specific information to select what are deemed "good" events, while FineProcess uses information between detectors to further refine the data. As of the time this document was written, the CoarseProcess involves a loose timing cut (window is 500 ns to 2500 ns) and a requirement that the FPGA did not fail. The FineProcess requires: accurate track matching (reduced χ^2 between 0.0 and 25.0), a beta cut ($0.0 < \beta < 1.2$), reasonable normalized calorimeter energy ($0.0 < \frac{E}{p} < 1.5$), and a suitable fractional momentum of the central value ($-20.0\% < \delta < 25.0\%$). Lastly, tracks through the focal plane are projected to the HGC mirror plane and a minimum NPE threshold is applied (NPE > 0.5) to generate the quantity NumTracksFired, counting how many "good" events had a track through the Cherenkov and registered a signal in the PMTs.

The calibration/efficiency script is found in hallc_replay/CALIBRATION/shms_hgcer_calib/calibration.C (or efficiency.C) and is formatted according to the TSelector framework for use in batch or in parallel using PROOF. As such, the script is broken into five components: Begin, SlaveBegin, Process, SlaveTerminate, and Terminate. Briefly: Begin outputs general information, SlaveBegin initializes histograms and logic conditions, Process acts as a sieve sorting replayed data into histograms, SlaveTerminate currently has no function, and Terminate does the actual fitting

and calibration from the histograms. The procedure for the use of these scripts is detailed in the README.md in the aforementioned directory.

2 Calibration Overview

Calibration is performed using two similar, but not equivalent, procedures. The first (hereafter called "quadrant" strategy) manually imposes tracking cuts on the CoarseProcess data to analyze what each PMT saw from each mirror quadrant. The second (known as "tracksfired" strategy) takes advantage of the FineProcess quantity NumTracksFired and performs cuts based on whether this quantity was incremented or not. Additionally, both strategies invoke identical cuts: both have a loose timing cut (1000 ns to 2000 ns), require there is only one valid reconstructed track, a beta cut ($(\beta$ - 1.0) < 0.2), and particle ID selection rules.

The goal of the calibration is to generate a reliable translation from the raw FADC channel to the physically meaningful number of photoelectrons (NPE). This is achieved by isolating the single photoelectron (SPE) peak to generate a scaling, then verify the scaling by calculating the linearity of the PE and their Poisson-like character.

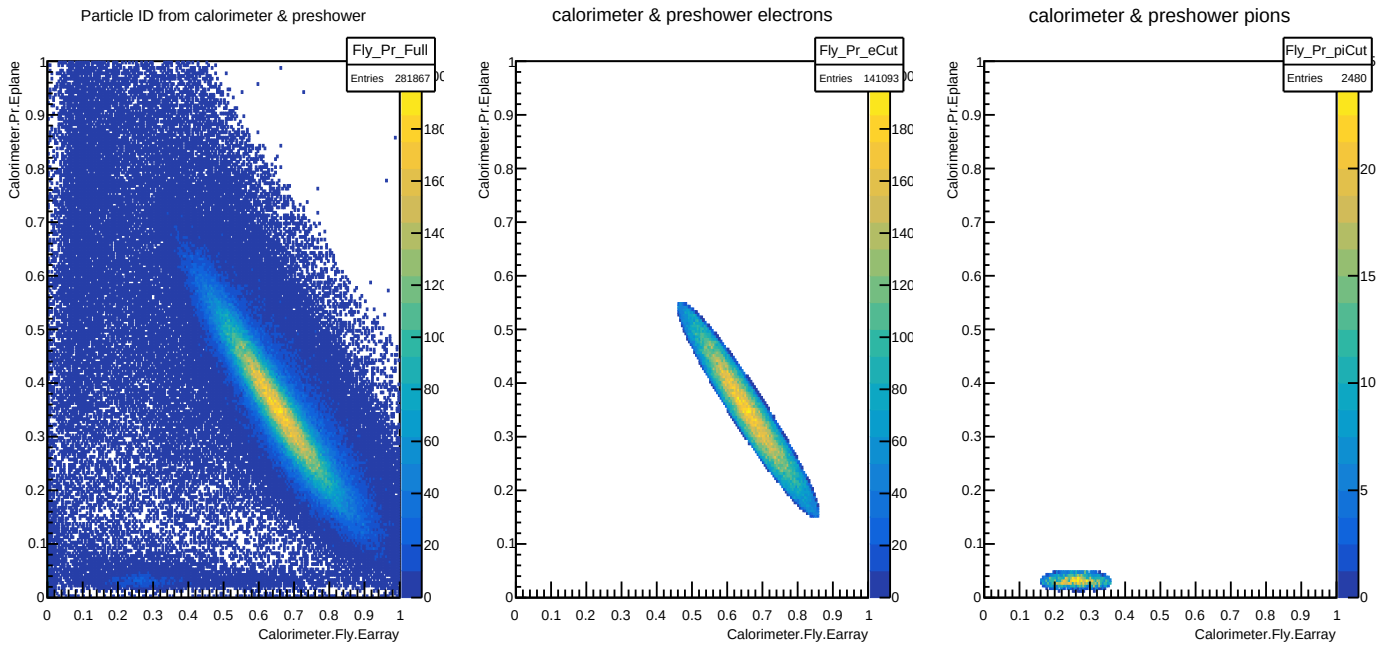

Figure 1: Particle ID for Cherenkov calibration. Shower and pre-shower are plotted on the x and y axes respectively and are used to separate electrons and pions. Left: Spectrum before any cuts; Center: Region of selected electrons; Right: Region of selected pions (π^-).

Before embarking on the specifics of each strategy, a brief digression into the particle ID procedure is given. As of now, only two particles are selected for, electrons and pions. They are chosen by plotting the energy of the "fly's-eye" calorimeter against the pre-shower. The resulting spectra (Figure 1) shows two distinct regions, the larger being electrons and the smaller pions according to the expected energy deposition of these particles. An elliptical cut is performed to select the appropriate regions according to the equation:

$$\frac{\left[(E_{\text{fly}} - x_{\text{center}})\cos(\theta) + (E_{\text{pre}} - y_{\text{center}})\sin(\theta)\right]^2}{a^2} + \frac{\left[(E_{\text{fly}} - x_{\text{center}})\sin(\theta) - (E_{\text{pre}} - y_{\text{center}})\cos(\theta)\right]^2}{b^2},$$

where a & b refer to the semimajor and semiminor axes, respectively and θ is the angle of rotation about the horizontal. A consistent theme in the calibration process is a large number of unexpected events, which can be seen in this spectrum as a significant smearing of the particle regions and localized regions of higher counts. It is strongly believed most of these events come from particles emitted from the target, and instead of traveling through the dipole as expected, bypass the magnet via a large gap in the detector hut entrance. Verification of this assumption will be performed in the 2017 Fall run, as this gap will be sealed by lead plates. For sake of argument, the large tail of the pion signal was tested for consistency with muon decay via the decay channel $\pi^- \rightarrow \mu^- + \nu_\mu$ with a central momentum of 3.0 GeV/c over a path length of 4.667 m (from end of dipole to HGC mirror plane) or 20 m (from target to HGC mirror plane) for a minimum/maximum muon estimate. The number of observed events are 300 - 500 in the pion tail while the muon estimate is 70 - 285, so it is unlikely that the tail is composed of muons.

The particle ID cuts are only used in the calibration to analyze the Poisson characteristics of the PMTs, since they are only expected to become apparent when electrons are selected for. In the efficiency section, the particle ID is used to determine the electron efficiency and pion contamination.

2.1 Quadrant Strategy

In this section, the Cherenkov analyzed is exclusively the HGC. However the procedure is applied to both detectors at the end.

As previously mentioned, this calibration strategy manually imposes the track matching logic post-replay and then locates the SPE. The track matching occurs in the Process stage and follows the simple equation,

$$x_{\text{HGC}} = x_{\text{Focal Plane}} + x'_{\text{Focal Plane}} * z_{\text{HGC}}$$

$$z_{\text{HGC}} = 156.27 \text{ cm},$$

with an identical form for the y dimension. This procedure yields 16 histograms, four PMTs receiving signals from four mirror quadrants. Since only the SPE is desired, the histogram corresponding to a PMT looking at its own mirror is ignored for now, as too much light drowns the SPE (for example, the signal PMT 1 sees from mirror 1 is too strong to isolate cleanly the SPE). These three histograms are fit with a Gaussian distribution about the SPE, and the mean of the three fits is taken to be the calibration. An illustration of the process is in Figure 2. The peak about channel 100 is attributed to vagrant particles entering the detector hut outside of the dipole. A previous presentation provides evidence for this conclusion[3]. Essentially, although this spurious peak survives timing, particle ID, and tracksfired cuts, identification of this peak as the SPE overestimates the expected NPE and introduces a large offset into the calibration. Since the pedestal removal has been accurate thus far, this conclusion is unacceptable. Therefore, it is assumed to be nothing but unwanted signal. Another explanation is cross-talk between the PMTs, but again this is unlikely since the peak is so uniform between all four.

After discussions with Pavel Degtiarenko[4], another possible source of this peak are photoelectrons failing to multiply properly at the first dynode. This could be due to non-uniformity of the dynode, edge effects, "almost elastic" collisions etc. Naturally, this interrupts the cascade effect and may lead to events in lower ADC channels. This is considered unlikely as well, due to the number of

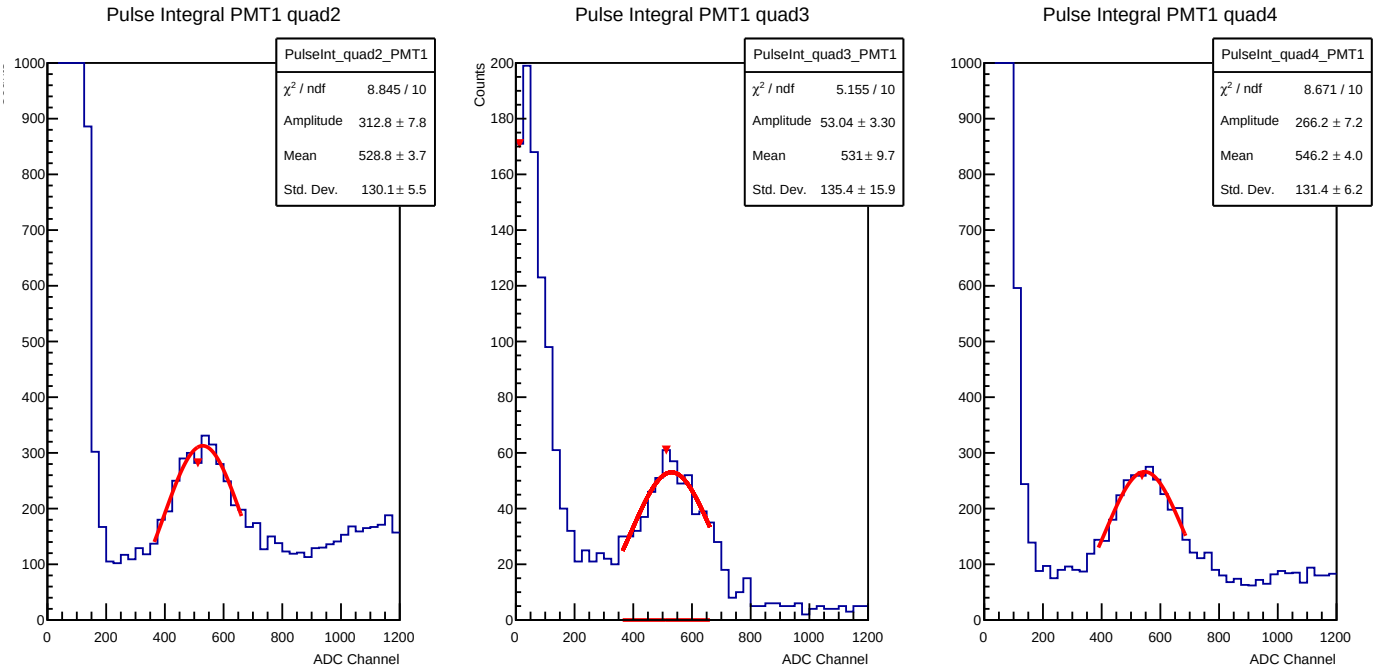

Figure 2: Illustration of locating the SPE in the HGC for PMT 1 FADC. Each plot shows the PMT pulse integral ADC for incident electrons in quadrants 2 - 4. The large peak near zero is believed to be particles passing though a gap in the detector hut shielding and not the true SPE. The SPE is fit with a Gaussian and the value of this mean is compared between quadrants for consistency. The red arrows are drawn by the peak finding algorithm, and so the second is taken to be the SPE.

events occupying the lower channels and their Gaussian distribution which is unexpected in stochastic processes. However, this hypothesis will be tested in the future by altering the gain of the PMTs.

In the case of low-statistics runs, there exist checks to ensure an accurate calibration is determined. Each fitted Gaussian is checked to ensure the peak has a minimum of 90 events, otherwise it is neglected (in Figure 2 the quadrant 3 fit is ignored). In case all three quadrants fail this statistics cut, all four quadrants are summed together and the procedure is repeated. Due to the shadowing of quadrant 4, as it is the furthest back, this happens most often with PMT 4. But when all remaining quadrants are combined, the SPE is clear, resulting in an accurate calibration.

With the calibration estimate obtained, new histograms are created to store the calibrated spectra of all four quadrants combined per PMT. This is achieved by filling this new histogram bin-by-bin by the previous histogram scaled by the obtained calibration value. In this way, each histogram can be given the same range and number of bins, facilitating combining all four PMT calibrations later. Figure 3 displays the resultant histogram. To verify the accuracy of the calibration, the linearity of the spacing between PE is investigated. In order to expose the second and third PE, a Poisson distribution is fit to the right hand side of the calibrated spectrum (the red fit in Figure 3) and subtracted off. This is done since at larger NPE the spectrum should be Poisson, so by subtracting off this contribution one is left with only the lower NPE. Once the first three PE peaks are resolved, the spectra is fit with a sum of Gaussians to determine their positions and therefore their spacing. An example of this procedure is shown in Figure 4.

From here, a second guess for the calibration constant is obtained by multiplying the calibration constant by the slope of the linear fit. The offset is ignored since it is essentially zero, and would imply a correction to the pedestal subtraction which is groundless. By doing this, the peak centered

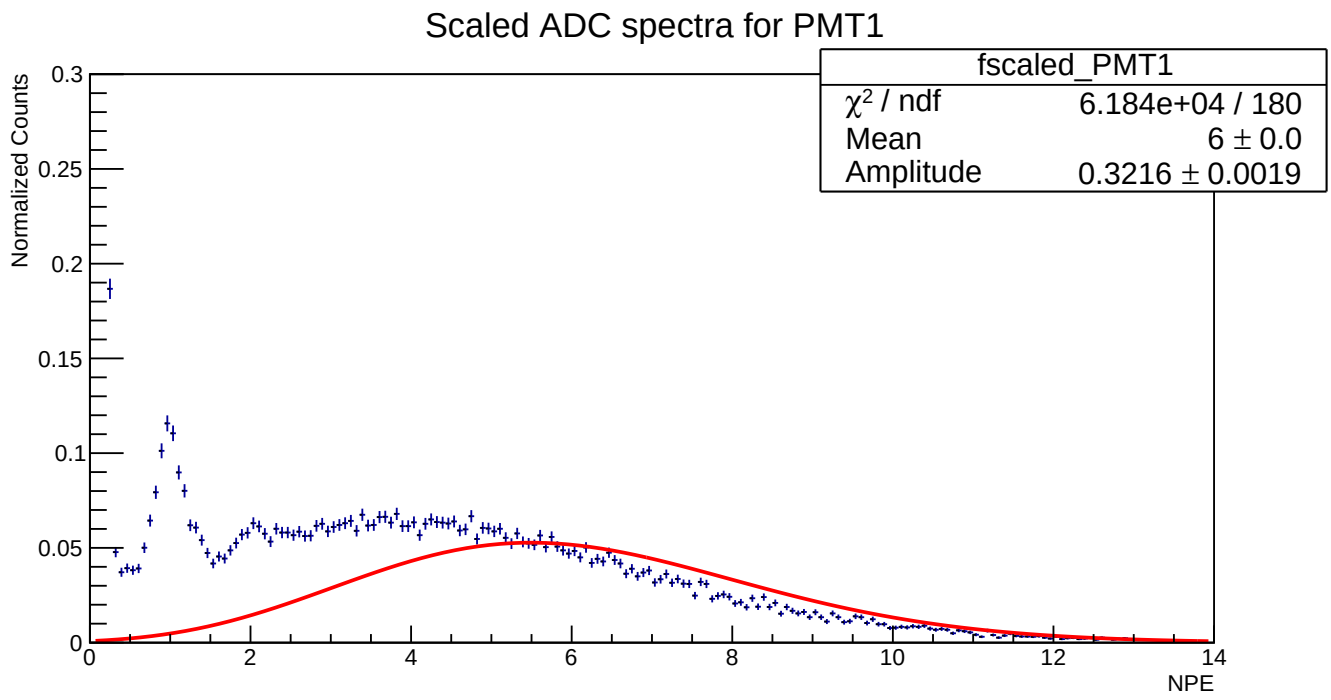

Figure 3: Result of calibrating a single PMT based of a Gaussian fit of the SPE. Note the peak chosen as the SPE can be seen to correspond to 1 PE. To facilitate the fitting of a Poisson distribution, the spectrum is normalized by its integral. The red curve is a Poisson distribution with $\mu = 6.0$ used to remove larger PE so the spacing can be determined.

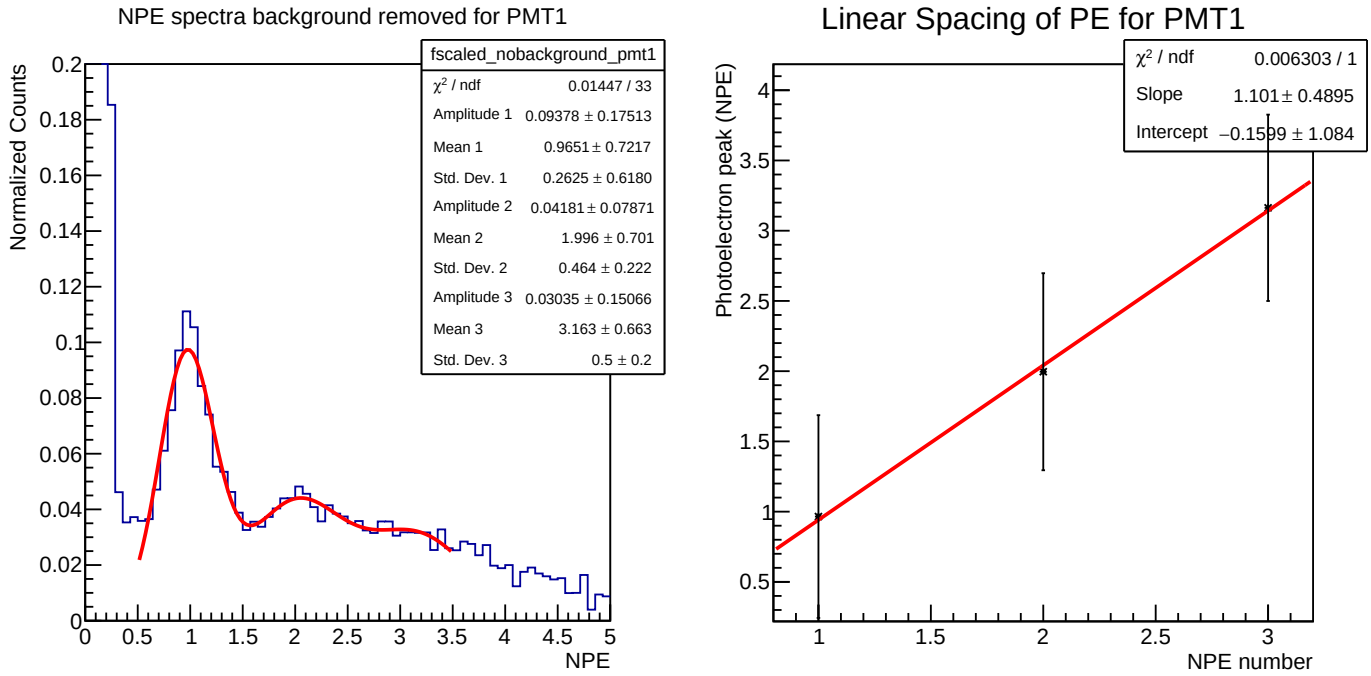

Figure 4: Result of subtracting off Poisson-like distribution at larger PE and the spacing of first three PE.

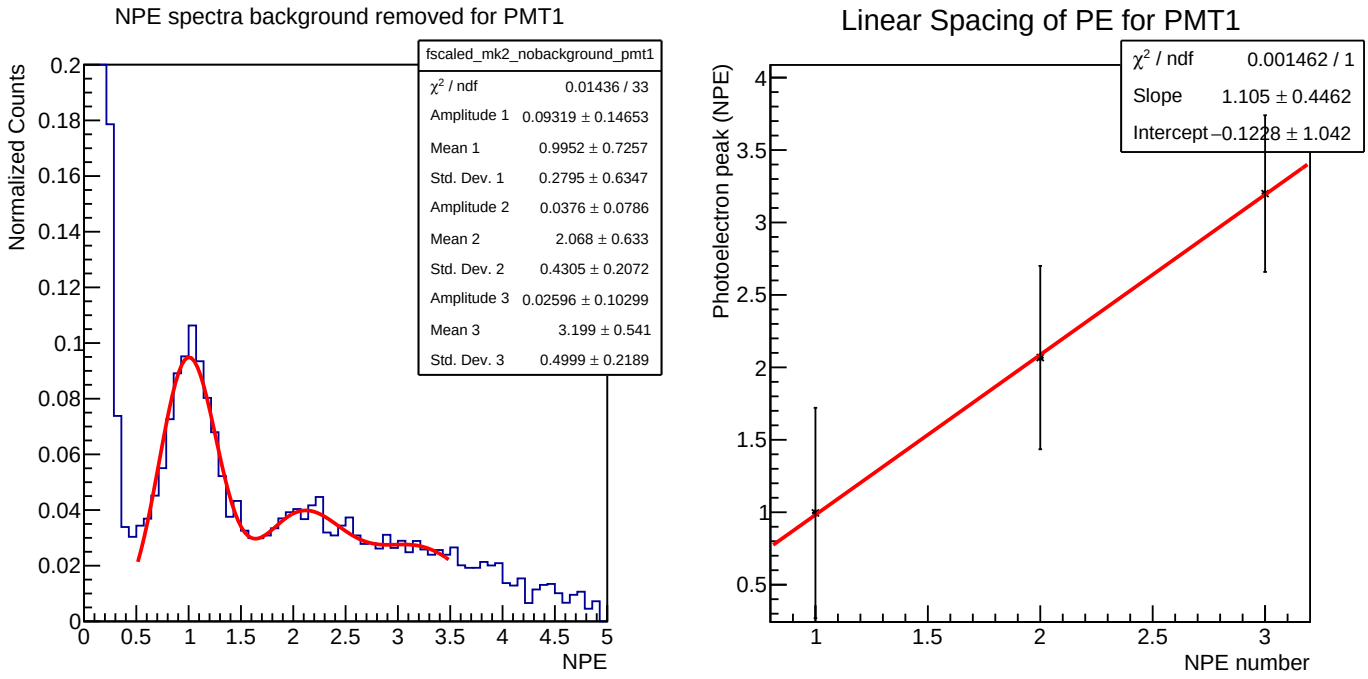

Figure 5: Second iteration of calibration constant. The updated calibration was obtained by multiplying the previous calibration constant by the slope of the spacing of the PE.

about one is expected to vary only slightly (since the slope is very close to one) while the spacing between PE may improve. With this new calibration constant, the same procedure is repeated and gives similar results, as can be seen in Figure 5. For reference, the two calibration constants calculated in this example are 538 ADC/PE for the first iteration and 541 ADC/PE in the second. Between the two fits, the better one is taken as whichever better predicts the SPE, i.e. for which the mean of the first Gaussian is precisely 1.0.

Another metric of goodness-of-fit is how well the calibration characterizes the expected Poisson nature of a properly calibrated detector. Here, all four PMTs are summed for each calibration selecting for electrons, and the resultant spectra are fitted with a Poisson distribution. Unfortunately, as Figure 6 shows, the HGC only observed an average of 5.0 PE with a larger number of SPE, which made calibration easy, but not possible to properly analyze high PE trends. It is anticipated that when the HGC is filled with C_4F_{10}, many more PE will be produced and the Poisson characteristics will become more lucid. As well, run 488 did not have properly tuned optics, and so the distribution is expected to improve in the future. The accuracy of the Poisson fit is determined by the reduced χ^2, and the calibration script outputs which calibration had a value closer to 1.0.

Table 1: Calibration Constants from Quadrant Strategy

	HGC		NGC	
PMT	Iteration 1	Iteration 2	Iteration 1	Iteration 2
1	525 ADC/PE*	487 ADC/PE	279 ADC/PE	323 ADC/PE*
2	412 ADC/PE	453 ADC/PE*	304 ADC/PE	379 ADC/PE*
3	362 ADC/PE*	438 ADC/PE	326 ADC/PE	431 ADC/PE*
4	488 ADC/PE	484 ADC/PE*	272 ADC/PE	292 ADC/PE*

Results of the quadrant calibration strategy. The better calibration is marked with an asterisk and is determined by the accuracy of the SPE. NGC calibration is measurably worse using this strategy since the SPE cannot be cleanly separated from the spurious peak about channel 100.

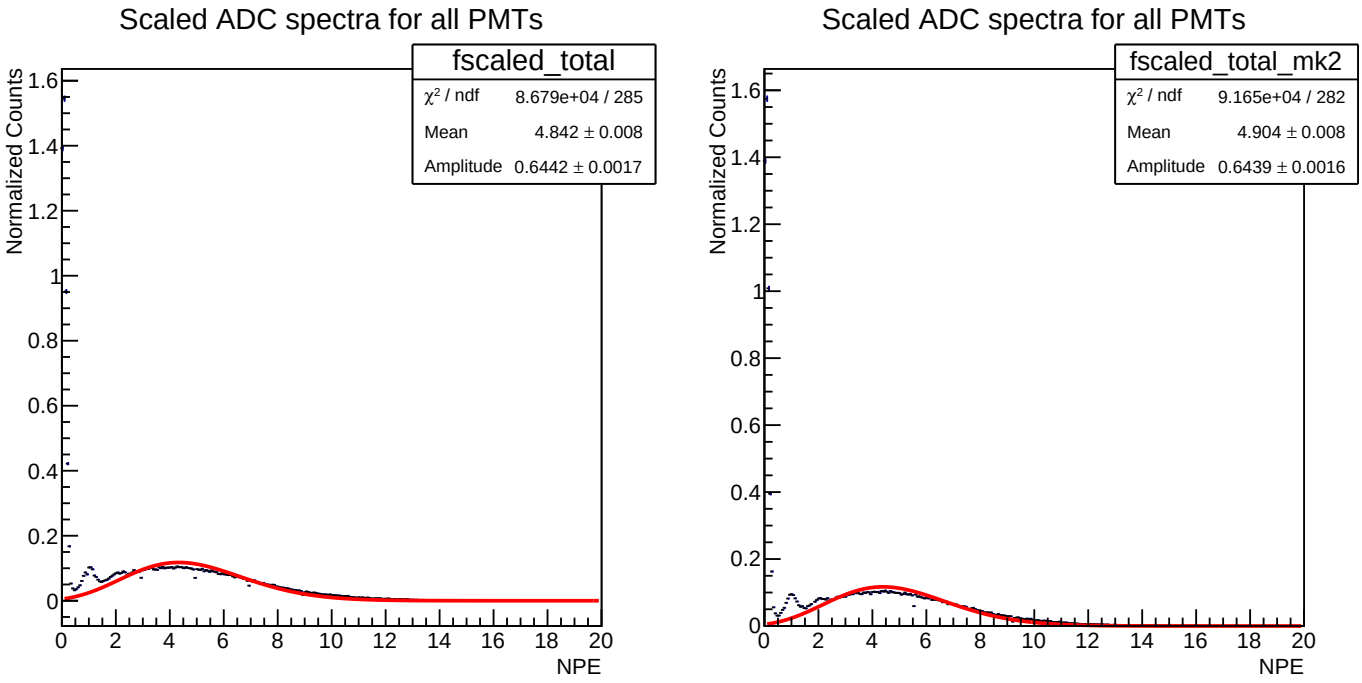

Figure 6: Poisson characteristics of the HGC with two different calibrations. Particle ID was applied to select for electrons.

2.2 TracksFired Strategy

In this section, the Cherenkov analyzed will exclusively be the NGC. However the procedure is applied to both detectors at the end.

For the tracksfired strategy the Process stage is simple; the only additional requirement is that numTracksFired != 0.0 which, as discussed in the Introduction, has implicit tracking and NPE cuts. From here, the procedure is similar to that of the previous strategy. Instead of each quadrant being analyzed, only the light the PMT receives from its own quadrant is processed. The other quadrants in this case have no useful information, as the large "junk" peak about channel 100 drowns out any SPE. As before, a peak finding algorithm locates the SPE, which is then fit with a Gaussian distribution, as can be seen in Figure 7. As before, this value is taken to be the first estimate of a calibration and the ADC channel is scaled appropriately. To determine the second guess, the previous method cannot be used, as it is too unreliable to isolate the second and third PE. Instead, the calibration constant is multiplied by the mean of a Gaussian fit of SPE, since this value should be close to 1.0. These methods are illustrated in Figures 8 and 9. Lastly, the same Poisson characteristics of the NGC are investigated in Figure 10. While it is promising at larger PE, the large source of SPE is present in this spectrum as well, which interferes with an accurate Poisson distribution. It is expected that both Cherenkovs will have better distributions as the optics are improved and the appropriate gases are added.

A further note about the Cherenkov calibrations, specifically the NGC, are the PMT gains. According to the HGC performance report the gains of the PMTs are expected to be twice as large as measured[5]. While this is not an issue with the HGC, if the NGC had double the gain the SPE may be resolvable since it will be distinct from the large "junk" peak. As of when this document was written, both the HGC and NGC have their raw analog signals enter a splitter in the Hall C counting house to allow the information to enter the trigger stream. This splitting accounts for the halving of the gain and may be replaced in future runs with a linear fan in/fan out. Although

this may introduce noise, ultimately the signal needs to be divided to get both TDC and FADC information.

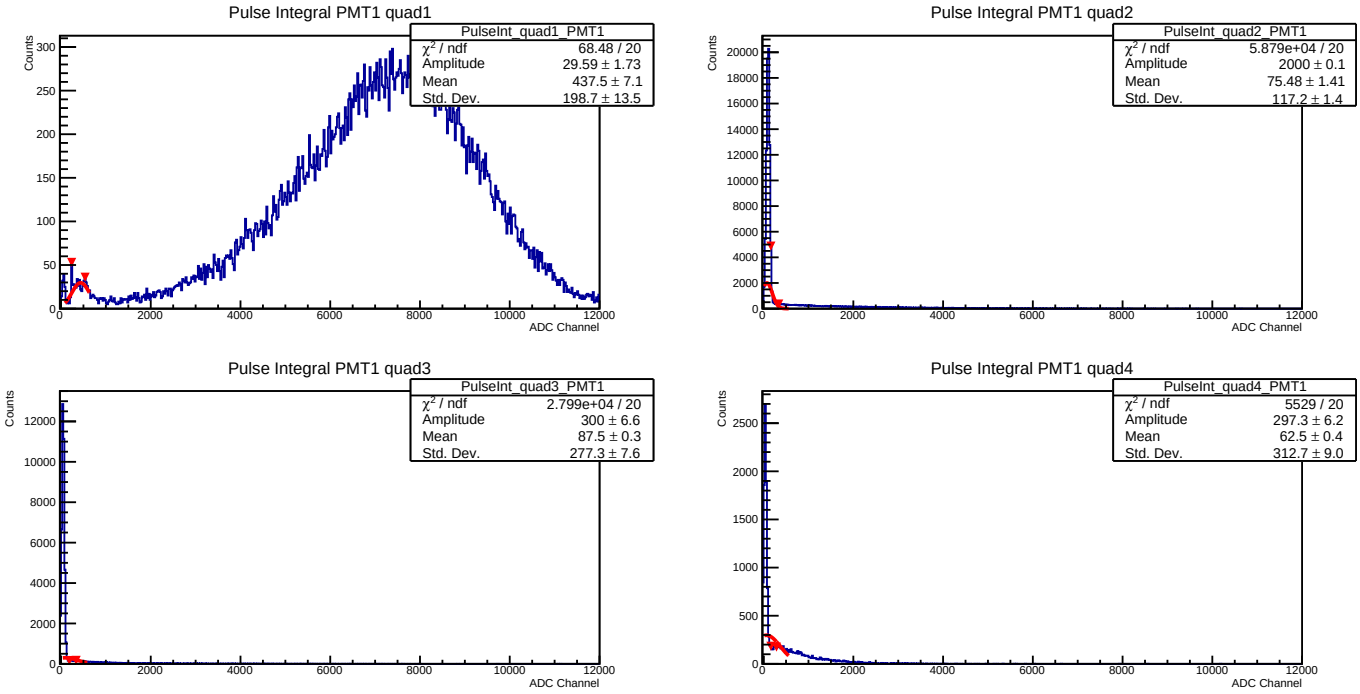

Figure 7: Illustration of SPE in NGC using tracksfired strategy. Each plot shows the signal received in each quadrant for PMT 1, where clearly the only acceptable SPE is in quadrant 1.

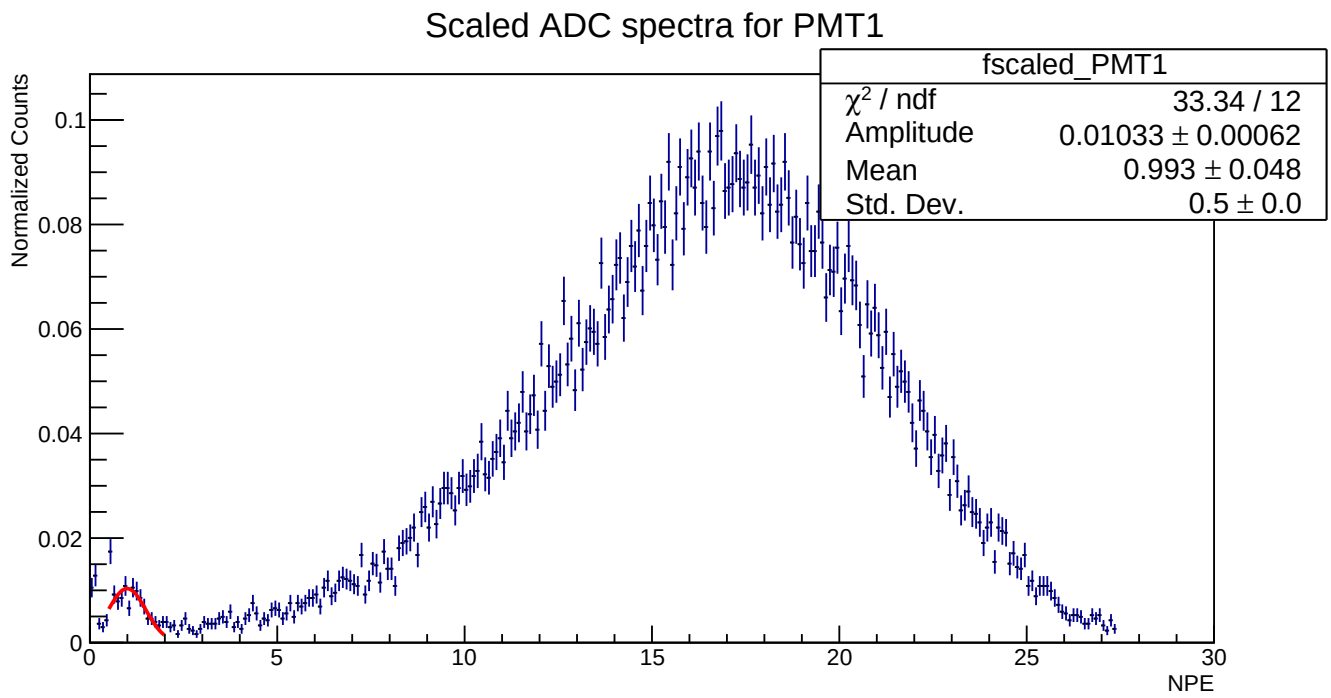

Figure 8: Result of calibrating a single NGC PMT. As with the HGC calibration, the spectrum is normalized to its integral. The red curve corresponds to a Gaussian fit of the SPE to determine goodness of calibration and to generate a second iteration.

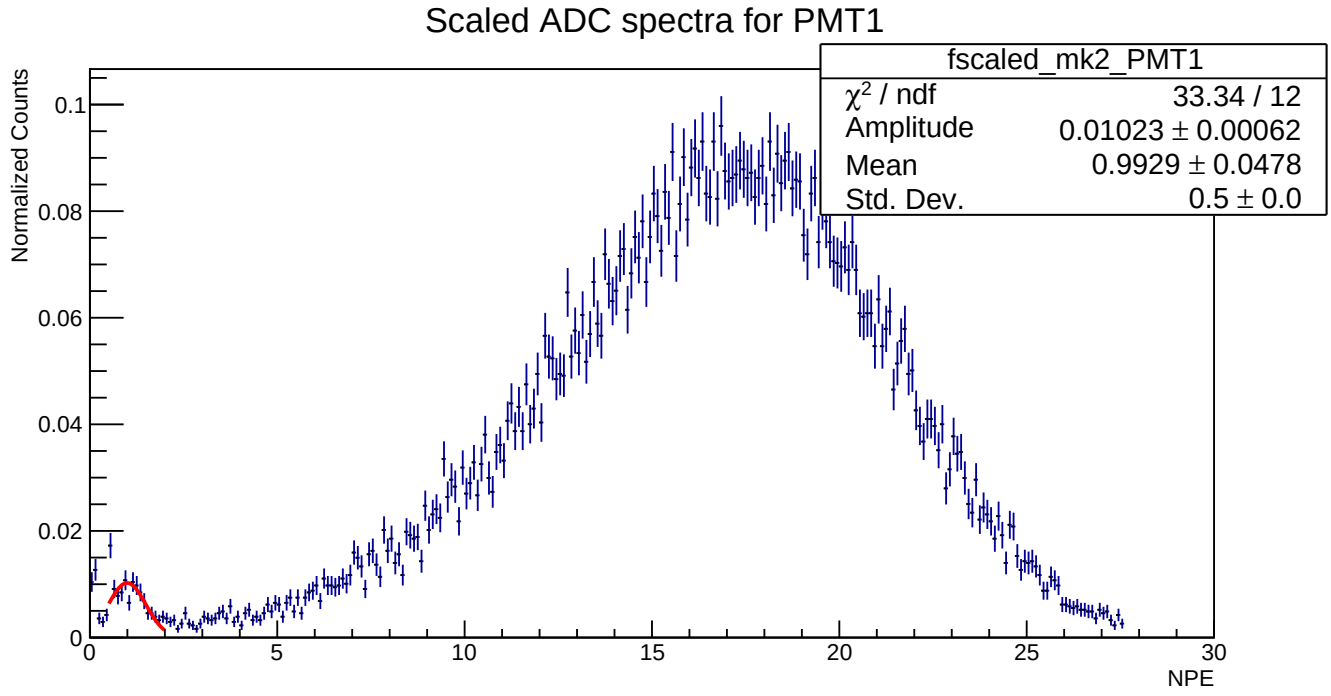

Figure 9: Second iteration of calibrating a single NGC PMT. The updated calibration constant is obtained by multiplying the previous with the mean of a Gaussian fit of the SPE. Here again the red curve is a Gaussian fit of the SPE used to determine goodness of the calibration.

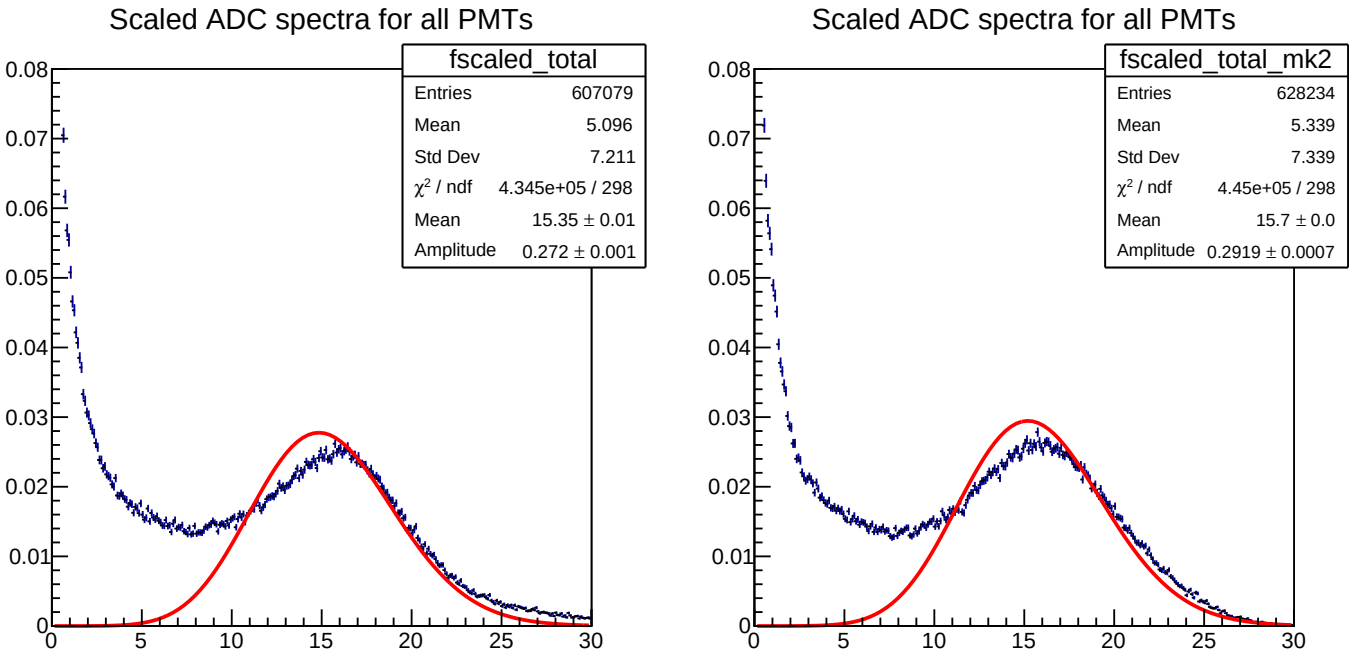

Figure 10: Poisson characteristics of the NGC with two different calibrations.

Table 2: Calibration Constants from Tracksfired Strategy

	HGC		NGC	
PMT	Iteration 1	Iteration 2	Iteration 1	Iteration 2
1	628 ADC/PE	848* ADC/PE	437 ADC/PE*	434 ADC/PE*
2	637 ADC/PE	956* ADC/PE*	436 ADC/PE	456 ADC/PE
3	587 ADC/PE	835* ADC/PE	433 ADC/PE*	376 ADC/PE*
4	481 ADC/PE	686* ADC/PE*	300 ADC/PE	411 ADC/PE

Results of the tracksfired calibration strategy. The better calibration is marked with an asterisk and is determined by the accuracy of the SPE. HGC calibration is markedly worse since the inherent PE cut in hcana removes some of the SPE.

3 Efficiency

The last stage of Cherenkov calibration is determining their efficiencies and the pion contamination. In this context, efficiency is how many electrons are correctly selected for a cut on NPE, while pion contamination is the number of pions that also pass this electron cut. In other words, pion contamination may be interpreted as the ratio of false positives to be expected. Therefore two quantities are reported: the electron efficiency which ideally is 100% and the pion contamination which ideally is 0. The efficiencies are calculated by taking the ratio of particles selected with the Cherenkov, divided by the particles selected without the Cherenkov:

$$efficiency = \frac{\text{[Particle ID][Tracks][Beta][Timing][TracksFired][Cherenkov]}}{\text{[Particle ID][Tracks][Beta][Timing][TracksFired]}} \times 100\%$$

Where quantities in brackets represent a cut. This quantity is strictly less than one and therefore can be expressed as a percentage. The pion contamination is a ratio as well:

$$\text{pion contamination} = \frac{[e^- \text{ efficiency}]}{[\pi^- \text{ inefficiency}]} = \frac{\text{\# of particles identified as electrons}}{\text{\# of pions incorrectly identified as electrons}}$$

Where this quantity goes to infinity if the pion inefficiency is 0 (if a pion is correctly identified every time, it will take an infinite number of electrons until a pion slips through).

Similarly to the calibration script, the efficiency script (efficiencies.C) adheres to the TSelector framework. In the Process stage the cuts applied are identical to those from before, with the addition of an optional cut on the other Cherenkov. In the Terminate stage the cut criteria are presented along with the results of the cuts on electrons and pions per PMT as well as for the whole detector. These results are shown in Figures 11 - 14. With these figures the definitions of electron efficiency and pion contamination are made clearer. For reference, the efficiency and contamination are shown on the next page. Several features of the efficiency calculation still require attention, such as localized inefficiency in some quadrants and lower than expected efficiency for the overall detector. It is expected the efficiency will improve greatly as the NPE increases and the uniformity will improve as the optics are calibrated.

Table 3: Efficiencies of Cherenkovs: NPE Cut at 2.0 & 1.5

NPE Cut	2.0				1.5			
Detector	HGC		NGC		HGC		NGC	
	e^- eff.	$\pi^- : e^-$	e^- eff.	$\pi^- : e^-$	e^- eff.	$\pi^- : e^-$	e^- eff.	$\pi^- : e^-$
PMT 1	85.90%	1:1568	99.90%	1:883	91.01%	1:1399	99.95%	1:500
PMT 2	91.95%	1:1754	98.84%	1:272	95.83%	1:1645	99.20%	1:244
PMT 3	90.87%	1:861	99.74%	1:2201	94.58%	1:701	99.85%	1:497
PMT 4	88.18%	1:895	98.50%	1:299	93.35%	1:782	99.16%	1:113
Full	89.79%	1:1142	99.37%	1:514	94.09%	1:985	99.59%	1:310

Results of the efficiency calculations. Electron efficiency is calculated by taking the ratio of the right and left plots in Figure 11 and Figure 12 for each PMT and the total detector. The pion to electron ratio is obtained by taking the ratio of the right hand plot in Figure 11 and Figure 12 over the right hand plot in Figure 13 and Figure 14 for each PMT and the whole detector.

Table 4: Efficiencies of Cherenkovs: NPE Cut at 1.0 & 0.5

NPE Cut	1.0				0.5			
Detector	HGC		NGC		HGC		NGC	
	e^- eff.	$\pi^- : e^-$	e^- eff.	$\pi^- : e^-$	e^- eff.	$\pi^- : e^-$	e^- eff.	$\pi^- : e^-$
PMT 1	95.16%	1:794	99.98%	1:233	98.41%	1:532	100.00%	1:133
PMT 2	98.36%	1:1055	99.54%	1:184	99.94%	1:715	99.82%	1:98
PMT 3	97.64%	1:357	99.92%	1:118	99.71%	1:216	99.97%	1:48
PMT 4	97.57%	1:394	99.52%	1:40	99.94%	1:268	99.84%	1:19
Full	97.41%	1:526	99.77%	1:131	99.60%	1:338	99.91%	1:61

Results of the efficiency calculations. Electron efficiency is calculated by taking the ratio of the right and left plots in Figure 11 and Figure 12 for each PMT and the total detector. The pion to electron ratio is obtained by taking the ratio of the right hand plot in Figure 11 and Figure 12 over the right hand plot in Figure 13 and Figure 14 for each PMT and the whole detector.

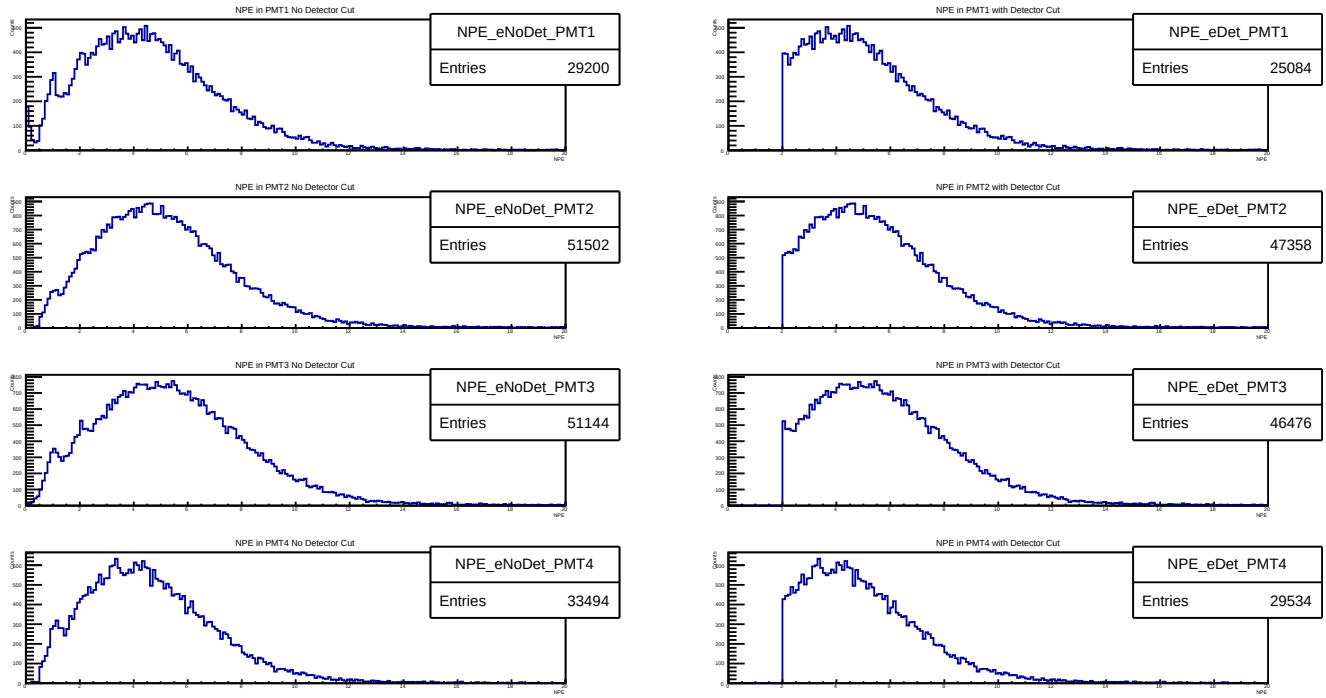

Figure 11: Spectra used to determine PMT electron efficiency. Each plot on the left corresponds to a PMT without any NPE cut while the plots on the right are PMT spectra with the NPE cut. Efficiency is determined by taking the ratio of the counts between each PMT.

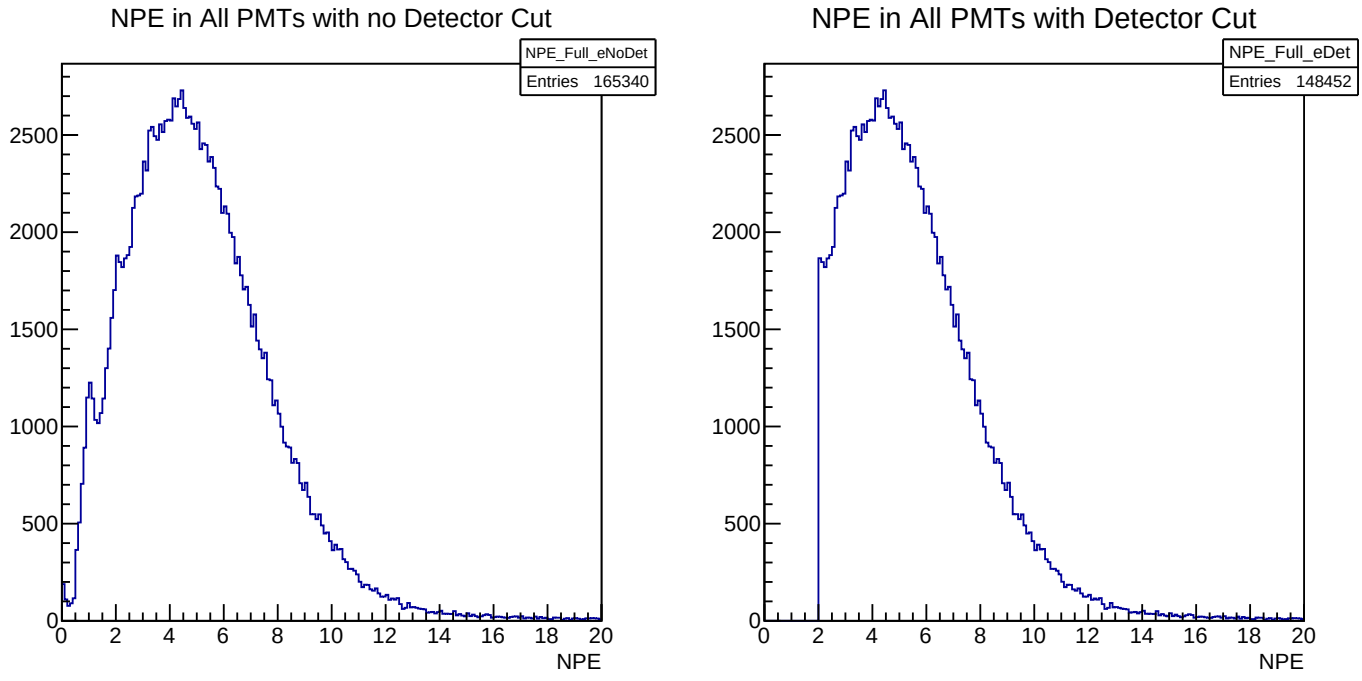

Figure 12: Spectra used to determine electron efficiency for entire Cherenkov detector. The left plot is the data without a NPE cut and the right plot is the data with a NPE cut. The efficiency is the ratio between the two spectra.

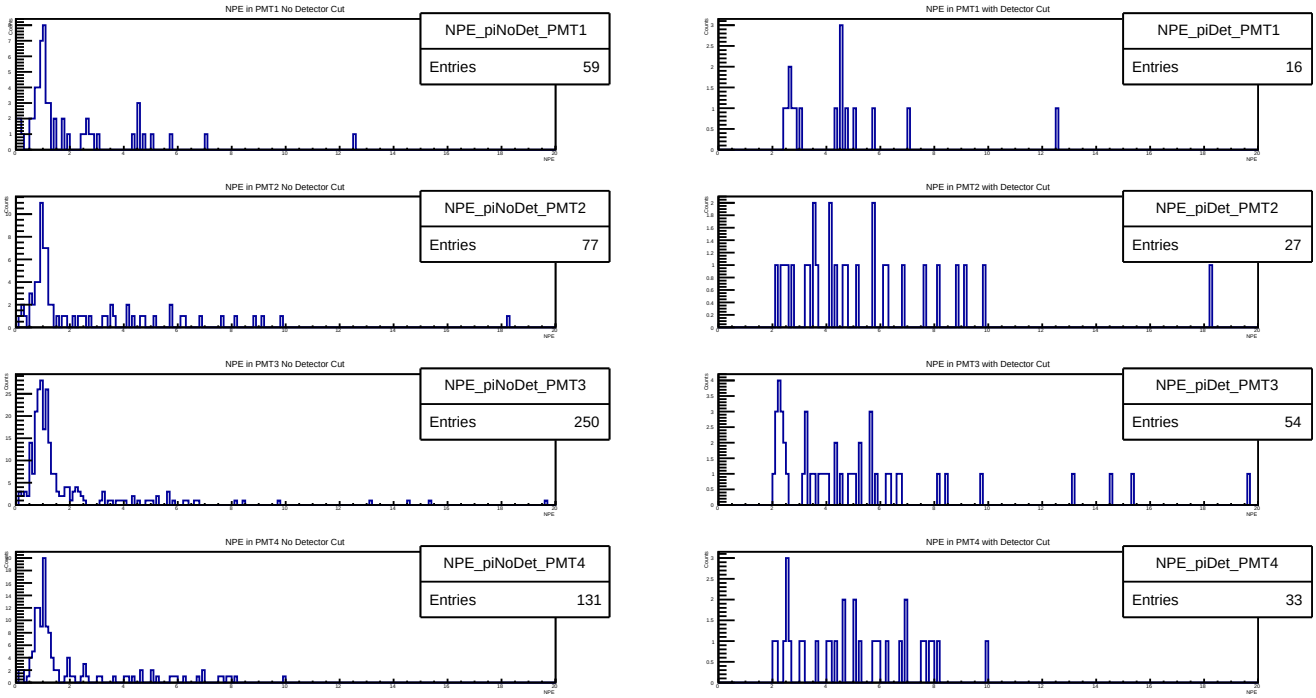

Figure 13: Spectra used to determine PMT pion contamination. Each plot on the left corresponds to a PMT without any NPE cut while the plots on the right are PMT spectra with the NPE cut. Contamination is determined by taking the ratio of particles identified as electrons over the number of pions identified as electrons between each PMT.

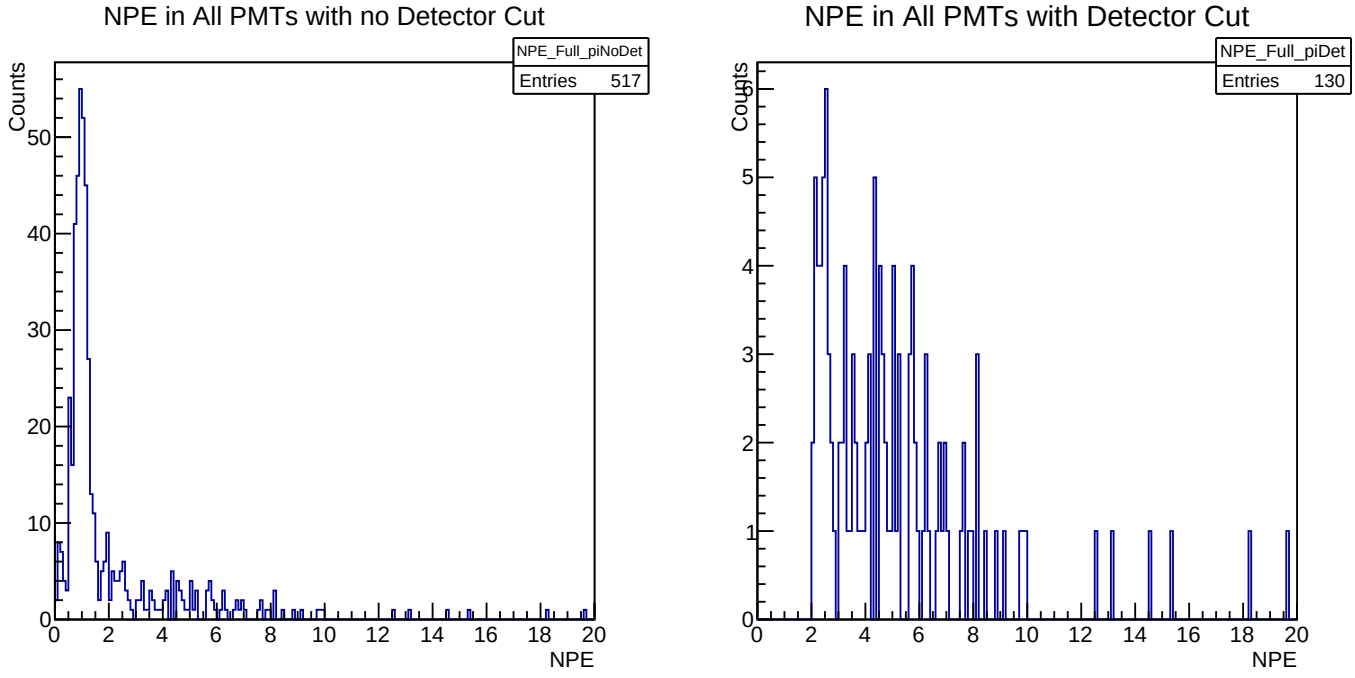

Figure 14: Spectra used to determine pion contamination for entire Cherenkov detector. The left plot is the data without a NPE cut and the right plot is the data with a NPE cut. The contamination is the ratio of particles identified as electrons over the number of pions identified as electrons.

References

[1] *Jefferson Lab Hall C Electronic Logbook*, Newport News, Virginia, https://logbooks.jlab.org/entry/3467029, 2017.

[2] *Jefferson Lab Hall C Electronic Logbook*, Newport News, Virginia, https://logbooks.jlab.org/entry/3467038, 2017.

[3] *Cherenkov Update (Run 488)*, Ryan Ambrose, University of Regina, https://hallcweb.jlab.org/DocDB/0008/000879/001/Detector_Slides.pdf, July 26 2017.

[4] Pavel Degtiarenko, Private Communication, August 28 2017.

[5] *Performance testing of 5 inch PMTs*, Alex Fischer, University of Regina, https://hallcweb.jlab.org/DocDB/0007/000738/001/gain_report.pdf, August 23 2012.